Erschienen in: Solar Energy Materials and Solar Cells ; 106 (2012). - S. 55-59
https://dx.doi.org/10.1016/j.solmat.2012.05.042

Time-resolved photoluminescence imaging with electronic shuttering using an image intensifier unit

David Kiliani *, Axel Herguth, Gabriel Micard, Jan Ebser, Giso Hahn

Universität Konstanz, Universitätsstr. 10, 78457 Konstanz, Germany

Keywords:
Photoluminescence imaging
Time-resolved
Lifetime
ICCD
Silicon

A B S T R A C T

In contrast to traditional steady-state photoluminescence imaging (PLI), time-resolved photoluminescence imaging (TR-PLI) allows for a calibration-free measurement of the effective transient minority charge carrier lifetime τ_{eff} in a silicon sample. For transient photoluminescence measurements, the illumination source as well as the camera signal have to be modulated on a time-scale in the order of τ_{eff}. Different approaches for camera signal modulation have been presented, including the use of a complementary metal-oxide-semiconductor (CMOS) camera or a rotating shutter wheel. In this work, the use of an InGaAs-based image intensifier unit as a fast optical shutter for TR-PLI was evaluated. Due to the fast switching times of the image intensifier, effective lifetimes down to 1/50 of the modulation period could be resolved reliably. Measurements under different illumination conditions allow for an injection-dependant analysis of τ_{eff} and comparison to photoconductance decay measurements.

1. Introduction

The spatially resolved determination of minority carrier lifetimes in silicon wafers is very important for the development of crystalline silicon solar cells, especially for multicrystalline material [1]. Camera based photoluminescence imaging (PLI) has proven to be a fast and reliable method for this task [2–4]. However, as a steady-state measurement technique, the correlation between measured PL intensity and effective minority charge carrier lifetime τ_{eff} has to be known for quantitative measurements. This correlation depends on many parameters, e.g., the optical properties of the sample surface, which may be laterally inhomogeneous and vary from sample to sample [5].

Transient lifetime measurements do not face this difficulty, as the absolute signal intensity is not relevant for the slope of excess carrier decay. As pump-probe measurements, they however require a modulated illumination and detection. It has been previously shown that using a CMOS camera [6] or a rotating shutter wheel [7–9], absolute lifetime values can be extracted from PL images. The use of an image intensifier unit as an alternative to the existing setups will be evaluated in this study. The image intensifier consists of a microchannel plate (MCP) photomultiplier and can be switched electronically, allowing global shuttering of the whole image area and eventually higher shutter frequencies. On the other hand, it may come at a significantly higher cost than the rotating mechanical shutter.

2. Measurement setup

A layout of the measurement setup is shown in Fig. 1. It contains two separate illumination sources: either backside illumination of the sample by an LED panel with a maximum photon flux of $2.6 \times 10^{17}\,cm^{-2}\,s^{-1}$ and a wavelength of 630 nm or illumination from the front using a homogenized laser beam with a maximum photon flux of $5.8 \times 10^{17}\,cm^{-2}\,s^{-1}$ and a wavelength of 808 nm. The PL signal was recorded with the intensified charge-coupled device (ICCD) camera C10054-15 from Hamamatsu Photonics.

This camera contains an image intensifier unit (consisting of MCP photomultiplier, photo-cathode and phosphorous screen) and a CCD image sensor, which are optically connected by a fiber coupling (see Fig. 2). The images were recorded at a resolution of 640×480 pixels. A non-standard InGaAs photo-cathode was used to make the camera sensitive to the spectral range of the silicon PL emission between 950 and 1250 nm. Electrons emitted from the photo-cathode are drawn to the MCP by a gate voltage and multiplied inside the channels by a further acceleration voltage, without losing the spatial information. The amplified bunch of electrons then hits a phosphorous layer and generates photons at 545 nm, which are recorded by the CCD camera sensor. The gate voltage between the photo-cathode and the entrance of the MCP can be modulated on the order of nanoseconds, which is the key

* Corresponding author. Tel.: +49 7531 88 3731.
E-mail address: david.kiliani@uni-konstanz.de (D. Kiliani).

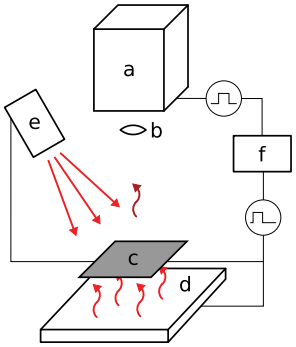

Fig. 1. Schematic measurement setup: The sample (c) is periodically illuminated by an LED panel (d) or a laser (e) and emits photoluminescence light. An ICCD camera (a) with an objective lens (b) is used to detect the PL radiation. The camera can be shuttered by the control electronics (e), which synchronize light source and image intensifier with an adjustable phase delay.

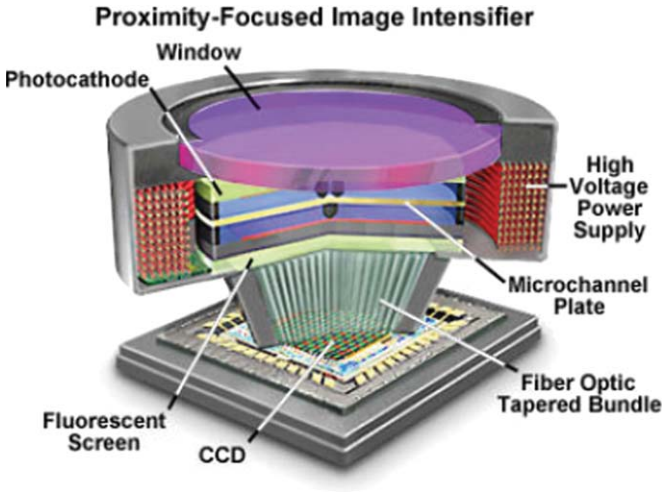

Fig. 2. Schematic layout of a fiber-coupled image intensifier unit (courtesy of Hamamatsu Photonics (http://learn.hamamatsu.com/articles/proximity.html)).

property of the camera system for this application as it allows the image intensifier to be switched between no transmission (gate voltage off or reversed) and full transmission (gate voltage on).

2.1. Measurement procedure

The sample was periodically illuminated for 50% of the period length T. The MCP gate voltage was switched on and off synchronously to the sample illumination with a defined phase delay φ, resulting in a shuttering of the recorded PL signal. To record the dynamic PL response of the sample to the periodic changes in illumination, several PL images with different phase delays φ were recorded. Due to the high amount of noise introduced in the AD-conversion of the analog video signal of the C10054-15 camera, comparatively long exposure times of 10–20 s per image were required even for high PL intensities. However, this is a limitation of the camera and could be avoided by using a camera with integrated digital readout.

A theoretical model (see [8]) was then fitted to the resulting φ-dependant PL intensity curve to obtain an effective lifetime value for each pixel. As the model assumes instantaneous switches between full illumination and no illumination, the slopes of the light sources have to be significantly shorter than the measured effective minority charge carrier lifetime τ_{eff} of the silicon sample. A fast Si photodiode with ns rise-time and a digital storage oscilloscope were used to measure the slopes shown in

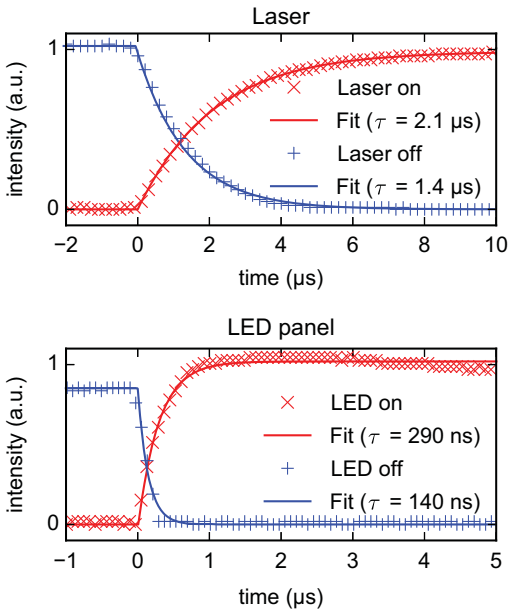

Fig. 3. Rising and falling slopes of the two light sources at full power. Note the different x-axis scalings. In order to quantify the switching times, the measured data were fitted with an exponential decay.

Fig. 3. Due to the smaller current of a diode string in the LED panel (< 100 mA) compared to the laser diode current (up to 10 A), the slopes of the LED illumination are shorter than the laser slopes.

3. Experimental results

To determine the lower limit of the lifetime measurement range, a 5×5 cm^2 area of an untextured, SiN_x passivated multicrystalline (mc) Si wafer with a thickness of 215 μm and $\sim 1\ \Omega$ cm p-type doping was measured. An excitation frequency $f_{\text{exc}} = 1/T = 2$ kHz was used, which is the maximum frequency of the C10054-15 ICCD camera. Image intensifiers supporting up to 200 kHz exist, but were not available for these measurements. The raw data for this lifetime map consist of 16 PL images taken at equidistant phase shifts $\varphi = 0 \ldots 2\pi$ with an exposure time of 20 s each. The sample was illuminated with the LED panel at a photon flux of 2.6×10^{17} cm^{-2} s^{-1}.

The lifetime image (Fig. 4a) generally correlates well with the steady-state PL intensity (Fig. 4b), except for the areas of lifetimes below ~ 7 μs. Here, the fitting of τ_{eff} to the measured data does not work reliably, due to the short lifetime values compared to the excitation period $T = 500$ μs and the low PL intensities. A map of relative uncertainties $\sigma(\tau_{\text{eff}})$ for the ICCD measurement is shown in Fig. 4c. It is based on the correlation matrix of the lifetime fit parameter at each pixel, taking into account the uncertainty of the measured PL intensities Φ due to photon shot noise ($\sigma(\Phi) = \sqrt{\Phi}$). Due to the strong electron amplification in the MCP, the noise contributions of the CCD sensor are negligible compared to the shot noise of the photo-electrons generated at the InGaAs photo-cathode [10].

Fig. 4d shows the relative uncertainty $\sigma(\tau_{\text{eff}})$ vs. τ_{eff}. As expected, the relative uncertainty is higher for small effective lifetimes. For the available f_{exc} of 2 kHz and ~ 1 sun illumination, effective lifetime values down to 10 μs can be measured with an average $\sigma(\tau_{\text{eff}}) < 10\%$. This is slightly higher than the previously reported 5 μs limit of the mechanically shuttered TR-PLI setup [9], obtained at $f_{\text{exc}} = 10$ kHz. A mechanically shuttered TR-PLI measurement of the same sample at 2 kHz yields a $\sigma(\tau_{\text{eff}}) < 10\%$ limit

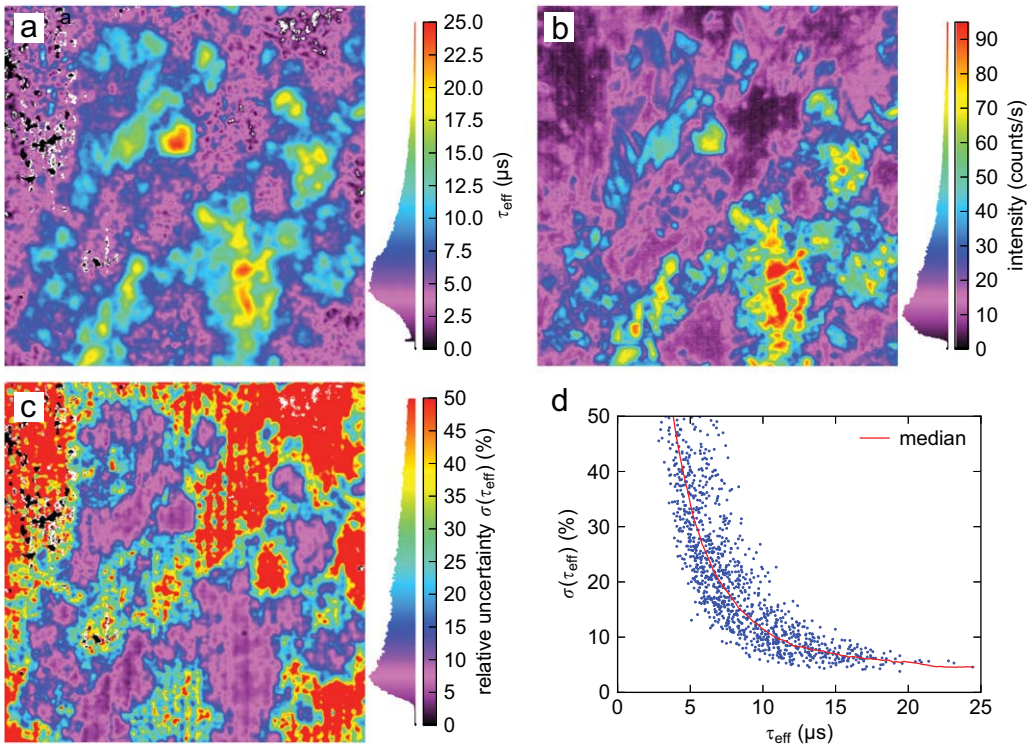

Fig. 4. (a) Transient lifetime map of a SiN_x passivated mc-Si wafer under LED illumination of 2.6×10^{17} cm^{-2} s^{-1} and 2 kHz excitation frequency. (b) Steady-state PL image of the wafer with identical illumination. (c) Relative uncertainty of the lifetime map (a). (d) Relative uncertainty vs. τ_{eff}: At $f_{exc} = 2$ kHz lifetimes down to 10 µs can be measured with $\sigma(\tau_{eff}) < 10\%$.

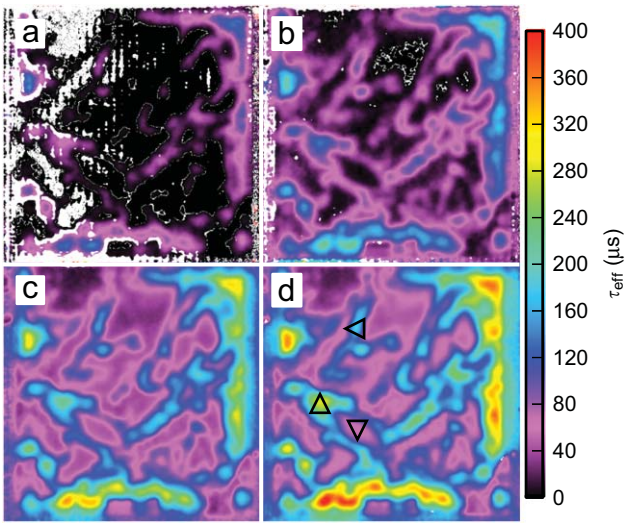

Fig. 5. Transient lifetime maps of an Al_2O_3 passivated 5×5 cm^2 mc-Si wafer at 2.5×10^{16} (a), 5×10^{16} (b), 1.5×10^{17} (c) and 2.6×10^{17} (d) cm^{-2} s^{-1} LED illumination. Pixels where the lifetime fit did not converge are shown in white. Three regions of different quality are marked in (d) for comparison with QSSPC (see Fig. 6).

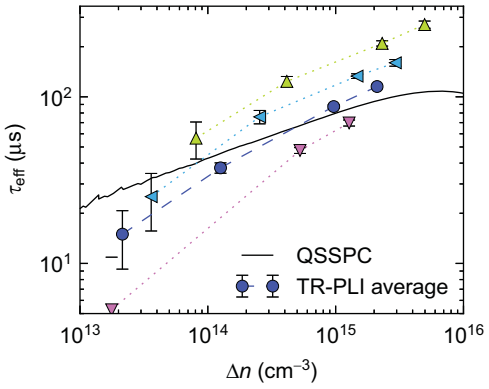

Fig. 6. Comparison of a QSSPC measurement and the lifetime values from TR-PLI for the wafer shown in Fig. 5. Circles mark the average TR-PLI lifetime over the sensitivity region of the QSSPC setup, triangles mark $\tau_{eff}(\Delta n)$ for the three regions indicated in Fig. 5d.

of about 17 µs. For an ICCD camera supporting higher repetition rates, significantly better lifetime resolution can be expected. However, comparably long integration times may be necessary due to the weak PL emission of low lifetime samples.

As τ_{eff} is usually a function of the excess charge carrier density Δn, the illumination conditions also have to be considered when measuring lifetime maps, especially for multicrystalline silicon.

Measurements with different illumination intensities and therefore different injection conditions were performed on an Al_2O_3 passivated 5×5 cm^2 mc-Si wafer with a thickness of $w = 100$ µm and $\sim 1\,\Omega$ cm resistivity. Fig. 5 shows the lifetime maps (a–d) for LED illumination with a varying photon flux.

The effect of different excess carrier densities on τ_{eff} can be clearly seen in these images. To compare the quantitative values to quasi-steady-state photoconductance [11] (QSSPC) measurements, the effective lifetime in three selected areas (marked in Fig. 5d) and the average lifetime over the sensitivity region of the QSSPC setup [8] was calculated for each of the TR-PLI lifetime maps. The results are shown in Fig. 6, together with a QSSPC measurement of the wafer. The QSSPC curve was obtained using a

Sinton Instruments WCT-120 lifetime tester in quasi-steady-state mode. The excess carrier density Δn for the PL measurements was calculated according to

$$\Delta n = G\tau_{\text{eff}} = E(1-R)\tau_{\text{eff}}/w, \quad (1)$$

where E is the incident photon flux and R is the reflectivity of the sample. Spectrophotometry yields a value of $R(630\ \text{nm}) = 32\%$ for the sample. The error bars indicate the 2σ confidence interval, with $\sigma(\tau_{\text{eff}})$ calculated as above.

For $\Delta n \approx 10^{15}\ \text{cm}^{-3}$ both methods agree very well. For lower injection, TR-PLI shows a steeper slope than QSSPC. This may possibly be explained by trapping of excited charge carriers [12] or the depletion-region modulation effect [13] due to the field-effect passivation of the sample. These effects lead to a higher QSSPC signal at low Δn but do not affect PL measurements [14]. Another possible explanation is the presence of a systematic error in the TR-PLI lifetimes, which could be caused by the fitting of very low PL intensities at low Δn: at low PL intensities, the relatively strong noise contribution may lead to peaks in the intensity curve and therefore an erroneous fitting of $\tau_{\text{eff}} = 0$ for some pixels. This can hardly be circumvented without relying on the absolute PL intensity value in the evaluation algorithm, which was intentionally omitted to keep the method calibration-free.

Several TR-PLI measurements at different illumination intensities E can also be combined into a map of τ_{eff} at a fixed Δn across the whole image by interpolating τ_{eff} along the Δn values from Eq. (1). This might be interesting for e.g., the determination of interstitial Fe concentrations [15]. A lifetime map for $\Delta n = 5 \times 10^{14}\ \text{cm}^{-3}$ is shown in Fig. 7. Some areas of the wafer with very low τ_{eff} could not reach this Δn even at full LED power and are therefore masked in white. Note that this kind of map cannot easily be obtained from other spatially resolved lifetime measurements like μ-PCD because of poorly defined injection conditions.

In order to compare the presented method with existing techniques, lifetime maps of the sample shown in Fig. 5 were recorded with four different methods (see Fig. 8). All measurements were done at ~ 1 sun illumination to be comparable to Fig. 5d.

A TR-PLI measurement with laser excitation at $2.1 \times 10^{17}\ \text{cm}^{-2}\ \text{s}^{-1}$ illumination (Fig. 8a) and $f_{\text{exc}} = 2$ kHz shows essentially the same result as the measurement with LED excitation in Fig. 5d.

The comparison to a TR-PLI measurement with a rotating mechanical shutter (Fig. 8b) and an excitation frequency of 2 kHz also shows very similar values. The mechanically shuttered measurement contains some areas where the lifetime fit did not converge (shown in white), which is probably caused by an uncertainty in the exact position of the fast moving shutter wheel and therefore the phase shift between shutter and excitation. As

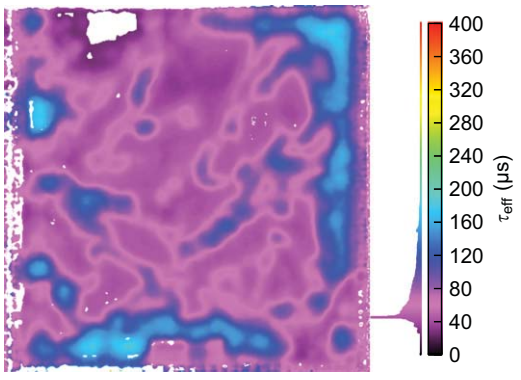

Fig. 7. Effective lifetime of the wafer shown in Fig. 5 at a fixed $\Delta n = 5 \times 10^{14}\ \text{cm}^{-3}$ for each pixel. Areas where this Δn could not be reached are shown in white.

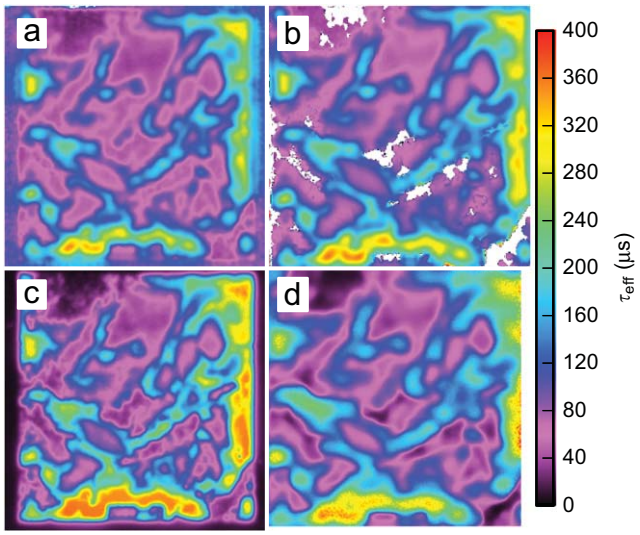

Fig. 8. Lifetime maps of the wafer shown in Fig. 5: (a) TR-PLI lifetime map with ICCD camera at $f_{\text{exc}} = 2$ kHz and laser illumination. (b) TR-PLI lifetime map with rotating mechanical shutter [9] at $f_{\text{exc}} = 2$ kHz and LED illumination. (c) Steady-state PL image calibrated with the measurement shown in Fig. 5d. (d) μ-PCD lifetime map.

the image intensifier unit is switched electronically with slopes in the low ns range, the phase shift is more defined for this shuttering technique.

A calibrated steady-state PL image recorded with the ICCD camera at $2.6 \times 10^{17}\ \text{cm}^{-2}\ \text{s}^{-1}$ LED illumination can also be used to obtain a lifetime map according to Eq. (1) and the radiative recombination equation

$$\Phi = A\Delta n(\Delta n + N), \quad (2)$$

where Φ is the PL intensity and N is the net doping concentration of the sample of $\sim 10^{16}\ \text{cm}^{-3}$. The calibration factor A was obtained using Eqs. (1) and (2) with the TR-PLI lifetime values τ_{tr} from Fig. 5d:

$$A = \Phi/G\tau_{\text{tr}}(G\tau_{\text{tr}} + N).$$

An average value of the resulting map of A over the sample area was then used to calculate Fig. 8c.

It is slightly more detailed and shows more contrast than the TR-PLI lifetime maps because the transient lifetime measurements are more affected by blurring due to PL light scattering and lateral carrier diffusion in the sample, leading to a reduced contrast in these images [16]. This effect can also be seen in the margin around the wafer edge, where the steady-state signal in Fig. 8c is nearly zero, whereas a TR-PLI measurement (e.g. Fig. 8a) reports the time-constant of the small amount of PL light from the wafer edge scattered at the suspending glass plate.

Microwave-detected photoconductance decay (μ-PCD) measurements were performed using a Semilab WT-2000 device. The μ-PCD lifetime map (Fig. 8d) also shows a very good correlation to Fig. 5d. However, due to the localized laser excitation and the measurement procedure of the μ-PCD setup, the exact injection level of (Fig. 8d) cannot be reliably estimated.

4. Conclusions

It was shown that TR-PLI measurements using an InGaAs micro-channel-plate photomultiplier as an electronic shutter are a feasible way to obtain quantitative lifetime maps of mc-Si wafers with high time-resolution. The fast global shuttering of the photomultiplier avoids sources of systematic error during the

calculation of the lifetime map from the recorded PL images and also avoids the rotating mechanical shutter. On the other hand, it may substantially increase the cost of a TR-PLI setup, compared to the mechanically shuttered approach.

Injection-dependant measurements on passivated mc-Si wafers show good agreement with QSSPC and μ-PCD lifetime values. Consistent results were obtained for laser and LED illumination, as well as for ICCD and mechanically shuttered recording. As the TR-PLI method provides the possibility of measuring $\tau_{\mathrm{eff}}(\Delta n)$ for each point of the sample, lifetime maps at a fixed Δn can be determined.

Acknowledgments

We would like to thank Hamamatsu Photonics for providing the camera used in this work. The financial support from the BMU project FKZ 0325079 is gratefully acknowledged, in particular for the processing and characterization equipment.

References

[1] B. Michl, M. Rüdiger, J.A. Giesecke, M. Hermle, W. Warta, M. Schubert, Efficiency limiting bulk recombination in multicrystalline silicon solar cells, Solar Energy Materials and Solar Cells 98 (2012) 441–447, http://dx.doi.org/10.1016/j.solmat.2011.11.047.

[2] T. Trupke, R.A. Bardos, M.C. Schubert, W. Warta, Photoluminescence imaging of silicon wafers, Applied Physics Letters 89 (4) (2006) 044107, http://dx.doi.org/10.1063/1.2234747.

[3] J.A. Giesecke, M.C. Schubert, B. Michl, F. Schindler, W. Warta, Minority carrier lifetime imaging of silicon wafers calibrated by quasi-steady-state photoluminescence, Solar Energy Materials and Solar Cells 95 (3) (2010) 1011–1018, http://dx.doi.org/10.1016/j.solmat.2010.12.016.

[4] S. Herlufsen, J. Schmidt, D. Hinken, K. Bothe, R. Brendel, Photoconductance-calibrated photoluminescence lifetime imaging of crystalline silicon, Physica Status Solidi (RRL)—Rapid Research Letters 2 (6) (2008) 245–247, http://dx.doi.org/10.1002/pssr.200802192.

[5] J.A. Giesecke, M. Kasemann, W. Warta, Determination of local minority carrier diffusion lengths in crystalline silicon from luminescence images, Journal of Applied Physics 106 (1) (2009) 014907, http://dx.doi.org/10.1063/1.3157200.

[6] S. Herlufsen, K. Ramspeck, D. Hinken, A. Schmidt, J. Müller, K. Bothe, J. Schmidt, R. Brendel, Dynamic photoluminescence lifetime imaging for the characterisation of silicon wafers, Physica Status Solidi (RRL)—Rapid Research Letters 5 (1) (2011) 25–27, http://dx.doi.org/10.1002/pssr.201004426.

[7] D. Kiliani, G. Micard, B. Raabe, G. Hahn, Time resolved photoluminescence imaging for carrier lifetime mapping of silicon wafers, in: Proceedings of the 25th EU PVSEC, Valencia, Spain, 2010, pp. 1363–1366. http://dx.doi.org/10.4229/25thEUPVSEC2010-2CO.4.2.

[8] D. Kiliani, G. Micard, B. Steuer, B. Raabe, A. Herguth, G. Hahn, Minority charge carrier lifetime mapping of crystalline silicon wafers by time-resolved photoluminescence imaging, Journal of Applied Physics 110 (5) (2011) 054508, http://dx.doi.org/10.1063/1.3630031.

[9] D. Kiliani, G. Micard, A. Herguth, G. Hahn, Progress in mechanically shuttered time-resolved photoluminescence imaging of silicon wafers, in: Proceedings of the 26th EU PVSEC, Hamburg, Germany, 2011, pp. 1463–1466. http://dx.doi.org/10.4229/26thEUPVSEC2011-2BV.2.20.

[10] D. Dussault, Noise performance comparison of ICCD with CCD and EMCCD cameras, Proceedings of SPIE 5563 (2004) 195–204, http://dx.doi.org/10.1117/12.561839.

[11] R.A. Sinton, A. Cuevas, M. Stuckings, Quasi-steady-state photoconductance, a new method for solar cell material and device characterization, in: Conference Record of the 25th IEEE Photovoltaic Specialists Conference, IEEE, 1996, pp. 457–460. http://dx.doi.org/10.1109/PVSC.1996.564042.

[12] D. Macdonald, A. Cuevas, Trapping of minority carriers in multicrystalline silicon, Applied Physics Letters 74 (12) (1999) 1710, http://dx.doi.org/10.1063/1.123663.

[13] P.J. Cousins, Experimental verification of the effect of depletion-region modulation on photoconductance lifetime measurements, Journal of Applied Physics 95 (4) (2004) 1854, http://dx.doi.org/10.1063/1.1638618.

[14] R.A. Bardos, T. Trupke, M.C. Schubert, T. Roth, Trapping artifacts in quasi-steady-state photoluminescence and photoconductance lifetime measurements on silicon wafers, Applied Physics Letters 88 (5) (2006) 053504, http://dx.doi.org/10.1063/1.2165274.

[15] D. Macdonald, J. Tan, T. Trupke, Imaging interstitial iron concentrations in boron-doped crystalline silicon using photoluminescence, Journal of Applied Physics 103 (7) (2008) 073710, http://dx.doi.org/10.1063/1.2903895.

[16] K. Ramspeck, K. Bothe, J. Schmidt, R. Brendel, Combined dynamic and steady-state infrared camera based carrier lifetime imaging of silicon wafers, Journal of Applied Physics 106 (11) (2009) 114506, http://dx.doi.org/10.1063/1.3261733.